Nonthermally Accessible Phase for CO on the Si(100) Surface

Deqing Hu* and Wilson Ho†
Laboratory of Atomic and Solid State Physics and Materials Science Center, Cornell University, Ithaca, New York 14853

Xiaojie Chen, Song Wang, and William A. Goddard III†
Materials and Process Simulation Center, Beckman Institute (139-74), California Institute of Technology, Pasadena, California 91125

(Received 28 August 1996)

A new phase *BT*-CO on Si(100), not accessible with thermal CO (which leads to the *T*-CO phase), has been observed using an energetic molecular beam of CO and characterized by first principles quantum chemical methods. The *BT* phase is composed of bridge (*B*) and terminal (*T*) sites; it is driven and stabilized by cooperative electrostatic interactions that result because *B* (*T*) binding leads to the transfer of charge *away from (toward)* the surface. Desorption of CO from the *B* site proceeds through the *T* configuration. [S0031-9007(97)02377-6]

PACS numbers: 82.65.Pa, 34.50.Dy, 68.45.Da, 82.65.My

We report here experimental and theoretical studies showing unusual and puzzling properties for the adsorption and desorption of CO on Si(100). We found that thermal CO leads to the *T*-CO phase in which there is one CO terminal bound to one Si of each dimer. However, translationally energetic CO leads to a new phase *BT*-CO, in which half the dimers have one CO symmetrically bound to both atoms of a dimer [bridge bound (*B*-CO)] while the other half have *T*-CO. This *BT*-CO phase is slightly more stable than *T*-CO.

The existence of such a surface CO phase not accessible to thermal experiments has not previously been reported, despite the numerous studies of carbon monoxide on metal [1] and semiconductor surfaces [2,3]. The formation of such thermally inaccessible phases might play a fundamental role in surface processes by which energetic barriers selectively promote the chemistry at specific sites. By increasing the translational energy and momentum of the molecule, additional chemical reaction pathways become accessible and new surface complexes can be formed. Transient enhancement of the mobility of the depositing species is also possible. These experiments provide detailed information concerning the potential energy surface of the gas-solid interface. In principle, these nonthermally induced chemical processes are relevant whenever the impinging species have excess translational energy. For example, hyperthermal energy particles are used for the growth and processing of thin films under conditions which differ importantly from techniques using thermal particles [4,5].

Previous experiments have shown [2,3] that CO readily adsorbs molecularly on Si(100) at <100 K, with a near unity adsorption probability. It has been postulated that CO molecules are weakly bonded to Si(100) in a head-on configuration with the CO axis nearly perpendicular to the surface (we refer to this as *T* for terminal).

By increasing the translational energy of CO incident on Si(100), we observed a new molecular CO state, in addition to the previously observed state. The upper panel of Fig. 1 shows electron energy loss (EEL) spectra of CO adsorbed on Si(100) at 85 K as a function of exposure to a 1.3 eV CO beam. The 261 meV EEL peak agrees with earlier experiments using ambient exposures from an effusive source and is interpreted as *T*-CO [2,3]. The

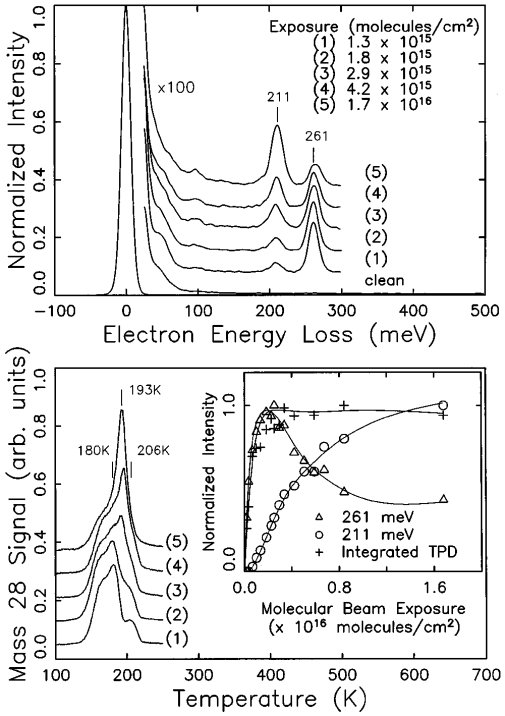

FIG. 1. High resolution electron energy loss spectra (Upper panel) and temperature programmed desorption spectra (Lower panel) after various exposures of Si(100) at 85 K to a 1.3 eV CO molecular beam. The TPD heating rate was 2 K s^{-1}. The spectra are offset for visual clarity. The Lower panel inset shows the normalized uptake of CO in the 261 and 211 meV states, and the total amount of CO as a function of exposure to the 1.3 eV CO beam.

 0031-9007/97/78(6)/1178(4)$10.00

EEL peak at 211 meV indicates the occurrence of a new CO adsorption state which we will interpret (*vide* infra) as *B*-CO. With increased CO exposure, the intensity of the 211 meV peak increases at the expense of the 261 meV peak. This change in the coverages of the two CO states is also reflected in the temperature programmed desorption (TPD) spectra associated with exposures to the 1.3 eV CO beam, shown in the lower panel of Fig. 1.

The CO uptake, shown as the inset in the lower panel of Fig. 1, is obtained by assuming that the coverages of CO associated with the 211 and 261 meV peaks are proportional to the normalized EEL intensities, while the total amount of CO adsorbed on Si(100) is proportional to the areas under TPD curves from 80 to 240 K.

The coverage of the 261 meV state quickly reaches a maximum and decreases, while that of the 211 meV increases steadily. The surface is initially saturated predominantly with the 261 meV state, and the total saturation coverage is independent of adsorption into the 211 meV state. Continued exposure to the energetic beam leads to a *T*-CO coverage of about half of the starting coverage, suggesting an equal amount of *T*-CO and *B*-CO. The adsorbed CO shows a significant redshift of the C-O stretch vibration in the new state; however, its desorption temperature remains low, near that of the other state.

When the substrate temperature was above 185 K no CO was observed in either the 211 or the 261 meV state, even with a large amount of 1.3 eV CO exposure. The TPD results show that 185 K is slightly higher than the desorption temperature of the 261 meV state ($\sim$180 K) while lower than the desorption temperature ($\sim$200 K) associated with the emergence of the 211 meV state.

If the surface is initially saturated with $^{12}C^{18}O$ through ambient dosing (261 meV state), followed with exposure to a 1.3 eV $^{12}C^{16}O$ beam, the TPD spectra clearly indicate co-adsorption of $^{12}C^{18}O$ and $^{12}C^{16}O$ in both the 261 and 211 meV states, with a reduction in coverage of the initially saturated $^{12}C^{18}O$.

By using either energetic N_2 or Ar in place of CO, we observed collision induced desorption of CO in the 261 meV state. However, the 211 meV state or the transformation of CO from the 261 meV state to the 211 meV state *was not observed* even with the chamber filled with 1.0×10^{-6} Torr of CO during energetic N_2 or Ar impingement.

The adsorption probability of CO in the 211 meV state depends on the translational energy of the incident molecule, as shown in Fig. 2 for CO incident perpendicular to the surface. A sharp rise in the adsorption probability was found to depend on the component of the energy normal to the surface, leading to an energy barrier of 0.9 eV for adsorption into the 211 meV state.

The simplest interpretation of these experimental results is that there is no barrier for CO to adsorb as *T*-CO but there is a 0.9 eV barrier to forming *B*-CO. The constant coverage of total chemisorbed CO as *B*-CO is formed indicates that there remains one CO per surface dimer.

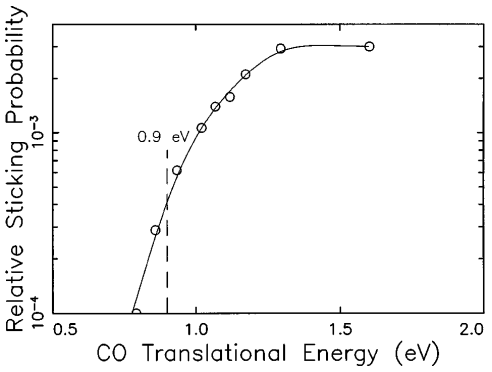

FIG. 2. The relative sticking probability in the 211 meV state as a function of translational energy of CO incident normal to the surface. An activation energy of 0.9 eV is deduced.

With continued exposure of the 1.3 eV CO beam, the *BT*-CO phase is formed.

The puzzles are as follows:

(1) If *B*-CO is more stable than *T*-CO, why does continued exposure to the energetic beam not lead to 100% *B*-CO?

(2) The desorption temperature for *B*-CO is very close to that for *T*-CO. The desorption of *B*-CO requires an energy of 0.55 eV (based on 200 K and a frequency factor of 10^{13} s^{-1}), while desorption of *T*-CO requires 0.50 eV (based on 180 K and a frequency factor of 10^{13} s^{-1}). However, formation of *B*-CO requires going over a barrier of 0.9 eV while formation of *T*-CO does not involve a barrier. These observations seem incompatible.

(3) Exposure to an energetic beam at 185 K does not lead to chemisorption, even though it is well below the desorption temperature of 200 K.

In order to help understand these results we carried out quantum mechanical [density function theory (DFT) and Hartree-Fock (HF)] calculations [6–8] on cluster models of the surface dimer and on periodic slabs [14,15], leading to the results summarized in Figs. 3 and 4.

For the isolated dimer we find an ordinary Si-Si sigma bond plus a weak π bond formed between the dangling bond orbitals of the two surface Si atoms. This leads to a slight distortion (5.7°) in the dimer. The dangling bond orbital on each atom combines to form two molecular

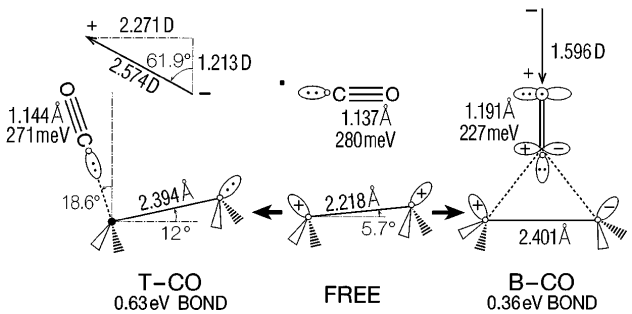

FIG. 3. Optimized structures, binding energies, vibrational energies, and dipole moments from DFT calculations on the CO/Si_9H_{12} cluster for terminal bound CO (*T*-CO), free cluster (FREE), and bridge bound CO (*B*-CO).

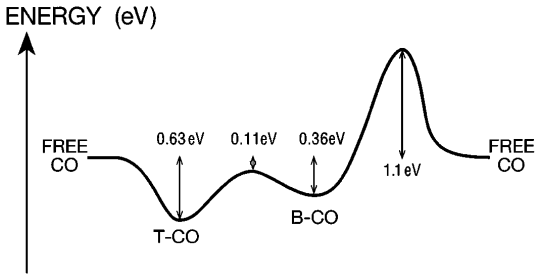

FIG. 4. Schematic showing the calculated binding energies and barriers for the CO/Si_9H_{12} cluster.

orbitals $d\pi$ and $d\pi^*$, where $d\pi$ is bonding and $d\pi^*$ is antibonding. The ground state of the dimer is the $(d\pi)^2$ singlet state. The $(d\pi^*)^2$ configuration leads to an energy calculated to be 0.59 eV higher (HF calculations).

Adding CO, we find that the most stable site is T-CO with a bond energy of $D = 0.63$ eV and a CO vibrational frequency of $\nu = 271$ meV. This agrees with EEL ($\nu = 261$ meV) and TPD ($D \sim 0.5$ eV) results on thermal CO. We find that the CO bonds to one surface Si atom, leading to an angle of 18.6° from the surface normal. The two electrons in the $d\pi$ Si-Si dimer bond are shifted strongly toward the second Si of the dimer, leading to a 12.0° tilting of the dimer. Concomitantly, the CO lone pair donates charge *into* the surface. There is no barrier for forming this state.

We also find a stable bridge state, B-CO, with a CO vibrational frequency of $\nu = 227$ meV, comparable with the observed value of $\nu = 212$ meV. We calculated a barrier of $E_{\text{bar}} = 1.1$ eV to form this state which is comparable with the observed barrier of $E_{\text{bar}} = 0.9$ eV. The origin of this barrier is associated with the nature of the bond. For B-CO we find that the ground state has $(d\pi^*)^2$ character in the Si-Si bond with delocalization (bonding) of $d\pi^*$ into the CO π^* orbital lying in the Si_2CO plane [think of it as a bond between Si_2 $(d\pi^*)^2$ and CO π^*]. The CO π bond in the plane then localizes more onto the oxygen, reducing the CO bond strength. This increases the CO bond distance from $R_{\text{CO}} = 1.14$ to 1.19 Å and decreases the CO frequency to $\nu = 227$ meV. The bonding of $(d\pi^*)^2$ to CO π^* leads to a charge transfer *toward* the CO.

Desorbing CO from B-CO while forcing it to remain along the surface perpendicular (and pointing to the Si-Si bridge position) leads to the $(d\pi^*)^2$ excited state of the free dimer. Bringing CO into the $(d\pi)^2$ ground state of the dimer leads to a repulsive energy curve. Thus we expect a significant barrier (calculated to be 1.1 eV).

However, starting with the equilibrium structure of B-CO and optimizing the geometry as one Si-CO bond is forced to increase from equilibrium ($R_{\text{SiC}} = 1.965$ Å) to infinity, we find (Fig. 4) that the B-CO dimer converts first to the T-CO configuration (with a barrier of 0.11 eV), which continues to dissociate with no barrier. Thus the desorption temperature should be similar for B-CO and T-CO.

These theoretical cluster results agree with the experiments, except *for one glaring discrepancy*. The B-CO bond strength is calculated to be 0.36 eV which is 0.27 eV *weaker* than the T-CO bond. Thus occupation of B-CO is surprising.

Because the charge transfers caused by T-CO and B-CO are quite different in character, we examined how the induced dipoles might couple [16]. Considering the dimer dipole as the reference, we find that B-CO induces a dipole moment of $\mu = -1.6$ D (*into* the surface, charge transfer away from the surface), while T-CO induces a dipole moment of $\mu = 1.2$ D (*out* of the surface, charge transfer into the surface) plus a component of $\mu = 2.3$ D parallel to the surface (oriented *along* the dimer toward the CO, charge transfer to the Si away from the CO). We did periodic lattice sums for different surface structures using these calculated induced dipoles, leading to the results in Table I; in summary:

(i) The T-CO phase leads to a $p(2 \times 2)$ structure with electrostatic effects responsible for *decreasing* the net cohesive energy by 0.09 eV (from 0.63 to 0.54 eV). This weakening of the bond is due to each CO having the same direction for the vertical dipole. The $p(2 \times 2)$ structure is preferred because the adjacent dimers have the surface-parallel dipoles in opposite directions, as illustrated in Fig. 5(a).

(ii) For B-CO the electrostatic effects *decrease* the cohesive energy by 0.19 eV, leading to $0.36 - 0.19 = 0.17$ eV.

(iii) For BT-CO the average bond energy (without electrostatics) would be 0.50 eV. However, arranging the B and T states in the $p(2 \times 2)$ structure shown in Fig. 5(b) leads to electrostatic interactions that *stabilize* this state by 0.06 to 0.56 eV.

The formation of the B-CO in the BT phase requires both a large activation energy plus the presence of nearby T-CO. This shows a twofold role for energetic CO.

TABLE I. Calculated cohesive energies for various unit cells of CO on Si(100). In each case there is one CO per surface Si-Si dimer. The single site energies are from DFT calculations on the dimer cluster (Si_9H_{12}). The induced dipole moments (directions noted by the arrows) were used in a two-dimensional lattice sum to obtain the total cohesive energies [16].

Phase	T	B	BT
Single site	0.63	0.36	0.50[h]
$p(2 \times 1)$	0.52	0.17	⋯
$p(4 \times 1)$	0.51[a]	⋯	0.44[d]
$p(2 \times 2)$	0.54[b]	⋯	0.56[e]
$p(4 \times 2)$	0.53[c]	⋯	0.56[f]
$p(4 \times 2)$	⋯	⋯	0.55[g]

[a] $(\vec{T} \quad \overleftarrow{T})$ [b] $\begin{pmatrix} \vec{T} \\ \overleftarrow{T} \end{pmatrix}$ [c] $\begin{pmatrix} \vec{T} & \overleftarrow{T} \\ \overleftarrow{T} & \vec{T} \end{pmatrix}$

[d] $(\overleftarrow{T} \quad B)$ [e] $\begin{pmatrix} \overleftarrow{T} \\ B \end{pmatrix}$ [f] $\begin{pmatrix} \vec{T} & B \\ B & \overleftarrow{T} \end{pmatrix}$ [g] $\begin{pmatrix} \vec{T} & \overleftarrow{T} \\ B & B \end{pmatrix}$

[h] Averaged over the T and B sites.

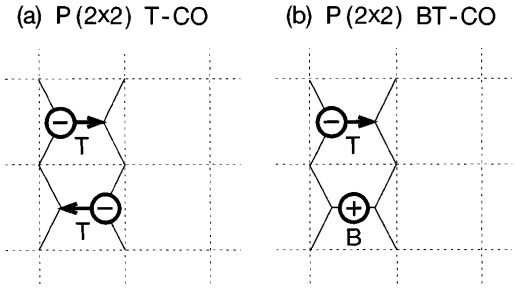

FIG. 5. Predicted optimum packing for CO on Si(100). (a) The $p(2 \times 2)$ structure for the T-CO phase, (b) the $p(2 \times 2)$ structure for the BT-CO phase. Each dashed square contains one Si dimer and one CO (circle). The $-$ $(+)$ sign shows a decrease (increase) of electron density on the CO; the direction of the arrow represents the direction of electron transfer between the Si atoms in the dimer.

First, it desorbs some T-CO, leading to empty dimer sites. Second, energetic gaseous CO can overcome the barrier at an empty dimer site to form B-CO. Continued exposure to energetic CO increases the population of B-CO defects in the T-CO phase to the point where there are sufficient defects to nucleate formation of the BT-CO phase. However, in order for an ordered phase to occur, the B-CO needs to migrate without actually diffusing or desorbing the bound CO molecules. We believe that, given a B-CO surrounded by T-CO molecules, there is a low barrier for one B-CO to convert to T-CO simultaneously with an adjacent T-CO converting to B-CO. Such a process is consistent with the isotope experiments described above. In this way, with a sufficient population of B-CO, the B-CO sites can aggregate to form the critical nucleus to transform to the new BT-CO phase with favorable dipolar interactions even though isolated B-CO is unstable with respect to isolated T-CO by 0.27 eV [17].

Note in Table I that three ordered BT structures have essentially the same energies; thus various domains may be present. Replacing one B-CO of the infinite BT lattice with T-CO is downhill by 0.14 eV [18], indicating that the BT phase is stable over a range of compositions. Electron diffraction and scanning tunneling microscopy studies should provide a test for these predictions.

We thank R. Hoffmann, Q. Liu, M. Teter, and B-L Tsai for valuable discussions. We gratefully acknowledge support of this research by the Air Force Office of Scientific Research Grant No. F49620-92-J-0309 (W. H.) and by the Office of Naval Research Grant No. N00014-95-F-0064 (W. A. G.). The facilities of the MSC are also supported by grants from DOE-BCTR, NSF (CHE-9522179 and ACR-9217368), Chevron Petroleum Technology Co., Aramco, Asahi Chemical, Owens Corning, Chevron Chemical Co., Chevron Research and Technology Company, Asahi Glass, BP Chemical, Hercules, Nippon Steel, and Beckman Institute. Some of the computations were carried out at the JPL Cray facility, the NSF Illinois Supercomputer Center (NCSA), and the NSF San Diego Supercomputing Center (SDSC).

*Present address: Hewlett-Packard Co., Corvallis, Oregon 97330.
†To whom correspondence should be addressed.

[1] J. T. Yates, Jr., Surf. Sci. **299/300**, 731 (1994).
[2] Y. Bu and M. C. Lin, Surf. Sci. **298**, 94 (1993).
[3] R. Y. Young, K. A. Brown, and W. Ho, Surf. Sci. **336**, 85 (1995).
[4] *Thin Film Processes II*, edited by J. L. Vossen and W. Kern (Academic Press, Boston, 1991).
[5] K. A. Brown, S. A. Ustin, L. Lauhon, and W. Ho, J. Appl. Phys. **79**, 7667 (1996).
[6] To model the Si(100) surface with a finite cluster we used Si_9H_{12} cluster model [7], with one pair of Si dimer atoms, each of which is bonded to two subsurface Si atoms. We carried out density function theory [8,9] calculations using the Becke parametrization for the density gradient corrections [10] in the electron-electron energy. The electronic correlation was described using the Perdew and Zunger [11] parametrization including relativistic effects [12]. For Si we used the scalar relativistic pseudopotential of Bachelet-Hamann-Schlüter [12] to replace the core electrons. The 631G** Gaussian basis set [13] was used for all atoms.
[7] A. Redondo, T. C. McGill, and W. A. Goddard, J. Vac. Sci. Technol. **21**, 344 (1982).
[8] M. N. Ringnalda *et al.*, PS-GVB 2.24 from Schrödinger Inc., 1996; B. H. Greeley *et al.*, J. Chem. Phys. **101**, 4028 (1994).
[9] W. Kohn and L. J. Sham, Phys. Rev. **140**, A1133 (1965).
[10] A. D. Becke, J. Chem. Phys. **98**, 5648 (1993).
[11] J. P. Perdew and A. Zunger, Phys. Rev. B **23**, 5048 (1981).
[12] C. B. Bachelet, D. R. Hamann, and M. Schlüter, Phys. Rev. B **26**, 4199 (1982).
[13] R. Krishnan, J. S. Binkley, R. Seeger, and J. A. Pople, J. Chem. Phys. **72**, 650 (1980).
[14] The DFT calculations using full periodicity were carried out with GDS-DFT [15]. These calculations used a repeated slab of six monolayers, each with a 2×2 surface unit and using the optimized structure from the cluster calculations.
[15] X. Chen, X. Hua, J. Hu, J-M. Langlois, and W. A. Goddard III, Phys. Rev. B **53**, 1377 (1996).
[16] In carrying out the electrostatic calculations, we first calculated the change in the induced dipole of an isolated cluster due to polarization of the semi-infinite surface. Using a dielectric constant of $\epsilon = 12.1$, we find that the perpendicular component is enhanced by a factor of 0.8 while the parallel component is reduced by the same factor.
[17] Starting with the T-CO phase and removing the first CO requires $0.63 - 0.19 = 0.44$ eV, while adding CO into the B state at this empty site gains $0.36 + 0.28 = 0.64$ eV.
[18] Replacing a single B-CO in the BT phase with a T-CO changes the energy by $\Delta E = (0.36 - 0.63) + (0.04 + 0.09) = -0.14$ eV.